Available online at www.sciencedirect.com
ScienceDirect
High Energy Density Physics 3 (2007) 297–301
High Energy Density Physics
www.elsevier.com/locate/hedp

X-ray polarization-dependent measurements of solid-density plasmas generated by fs laser pulses

F. Zamponi [a,*], A. Lübcke [a], T. Kämpfer [a], I. Uschmann [a], E. Förster [a], R. Sauerbrey [a,1], B. Hidding [b], M. Clever [b], G. Pretzler [b], E. Kroupp [c], E. Stambulchik [c], D. Fisher [c], Y. Maron [c], R. Sharon [d], M. Deutsch [d]

[a] X-Ray Optics Group, Institute for Optics and Quantum Electronics, Friedrich-Schiller-Universität Jena, Max-Wien-Platz 1, 07743 Jena, Germany
[b] Institut für Laser- und Plasmaphysik, Heinrich-Heine-Universität Düsseldorf, Universitätsstrasse 1, 40225 Düsseldorf, Germany
[c] Faculty of Physics, Weizmann Institute of Science, Rehovot 76100, Israel
[d] Physics Department, Bar-Ilan University, Ramat-Gan 52900, Israel

Available online 8 February 2007

Abstract

We report on studies of plasmas, formed by the interaction of 80 fs, 1 J Ti:Sapphire laser pulses with solid matter. The laser intensity was 5×10^{19} W/cm^2. The $K_{\alpha 1,\,2}$ X-ray emission spectra at $\approx$4.5 keV were measured using a toroidally bent GaAs (400) crystal spectrometer with the spectral and spatial resolutions of 0.3 eV and 4 μm, respectively. A Si (220) polarizer was used for determining the polarization properties of the recorded emission. A strong polarization dependence of the K_α satellite emission was observed, which may indicate an anisotropy of the relativistic electron velocity distribution. Also, electrons with energies in the range of 500 keV–13 MeV were detected using an electron spectrometer.

PACS: 52.38.Fz; 52.50.Jm

Keywords: Laser–plasma interactions; Polarization spectroscopy; Line profiles

1. Introduction

Spectropolarimetry allows detailed measurement and analysis of radiation, as well as its interaction with matter. Polarized spectra are sensitive to anisotropies in the radiating and transmitting media, such as directionality in the electron velocity distribution [1]. Such polarization-dependent measurements have been employed in studies of the laser–plasma interaction [2,3], in high resolution X-ray spectroscopy of trapped ions [4,5] and of X-pinch [6].

K_α emission in a target, produced by electrons accelerated in a dense, thin plasma layer at the target surface by laser pulses, can be used to monitor the interaction between electrons and matter [9]. Spectropolarimetry of the K_α emission allows the study of the behavior of electrons *inside* the target. Compared with other techniques, this is a clear advantage. For example, an electron spectrometer measures the energy of electrons *after* they exit the target. In between they traverse huge electric fields, of the order of TV/m [10], created by the space charge separation. Thus, the electron spectrum may be altered considerably. Alternatively, a layered target can be used, in conjunction with an imaging system, to monitor the K_α emission from the different layers [11,12]. This method also has drawbacks: the cross-section for the K-shell ionization by electron impact is not a monotonic function of the energy. For example, for titanium it has a maximum at 20–30 keV, then a fall-off, and again a rise at MeV energies. In looking at the emitted intensity, it is not possible to determine whether it was generated by the high-energy electrons, going in the forward direction, or by electrons with much lower energy forming the return currents.

* Corresponding author.
E-mail address: zamponi@ioq.uni-jena.de (F. Zamponi).
[1] Present address: Forschungszentrum Dresden, Bautzner Landstrasse 128, 01328 Dresden, Germany.

1574-1818/$ - see front matter © 2007 Elsevier B.V. All rights reserved.
doi:10.1016/j.hedp.2007.02.029

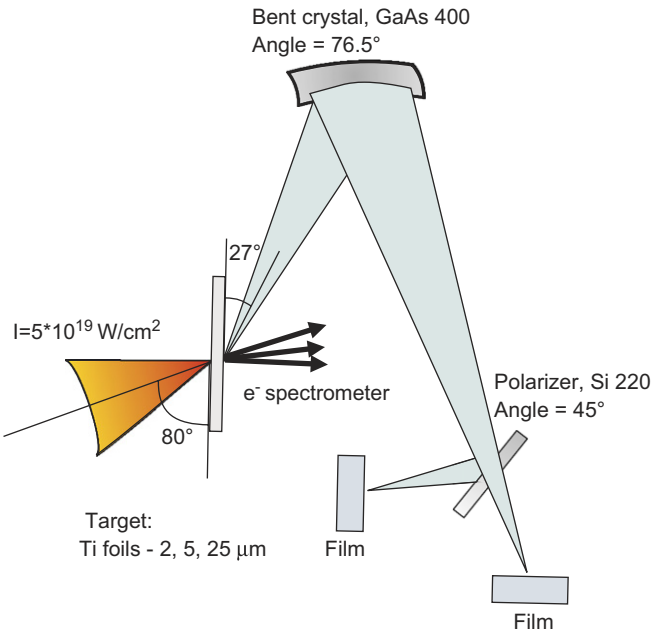

Fig. 1. A scheme of the experimental setup (color in online).

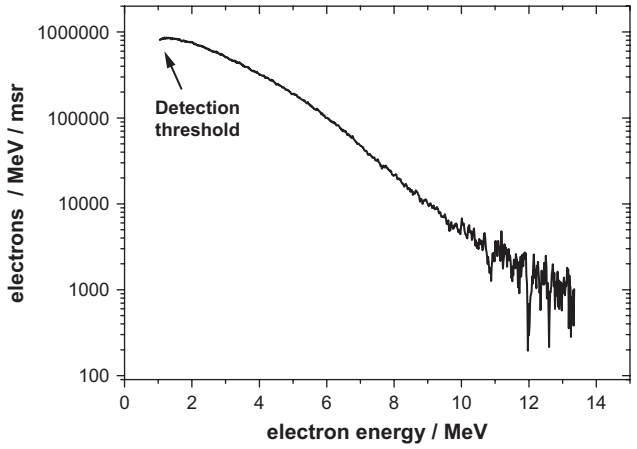

Fig. 2. A typical electron spectrum.

2. Experimental setup

The experiments were performed at the JeTi, the Jena multi-TW Ti:Sapphire chirped-pulse-amplified laser system [13]. The experimental setup is given in Fig. 1. The system consists of an oscillator, a stretcher, a regenerative amplifier, two additional multi-pass amplifiers, and an in-vacuum compressor. The maximum energy output before compression is 1.3 J, giving about 0.7 J after compression, with a pulse duration of 80 fs at a repetition rate of 10 Hz. After the compression, the laser beam is guided to the target chamber through a vacuum beam-line to avoid a nonlinear interaction of the laser pulse with the atmosphere. In this study, the maximum energy transmitted to the target was 600 mJ. In the target

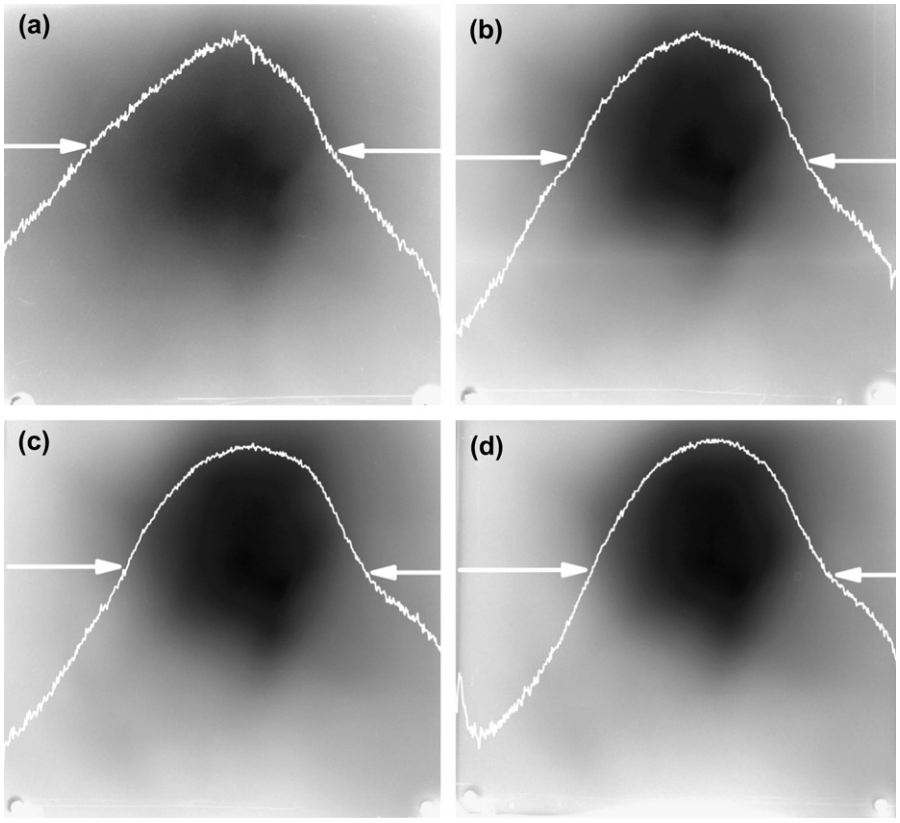

Fig. 3. Image plates forming the sandwich Al filter/image plate used to measure the divergence of the electron beam emitted in the forward direction. (a) Denotes the image plate closest to the target.

chamber the beam is focused by an off-axis parabolic mirror onto a foil target to focal spot sizes down to 5 μm^2, yielding intensities from 10^{18} to 5×10^{19} W/cm^2, by varying energy and pulse duration. Titanium foils 25, 5, and 2 μm thick were used as target. Behind the target an electron spectrometer was assembled as an additional diagnostic. Alternatively an image plate stack could be employed to monitor the total amount of electrons, their energy and directionality.

The X-ray spectrometer employed a GaAs (400) crystal toroidally bent to radii of 450 mm in the horizontal direction and 305.9 mm in the vertical direction. It had an energy resolution $E/\Delta E \approx 15000$ and a spatial resolution in the vertical direction of 20 μm in the first experiment, and, using a higher crystal quality, 4 μm afterwards. A flat Si (220) crystal polarizer could be positioned in a non-dispersive orientation downstream from the bent-crystal analyzer, to allow the acquisition of polarized spectra. The polarizer is coupled to the spectrometer in a non-dispersive setup [14]. The spectrum was recorded by means of Agfa Structurix X-ray film, which was calibrated in intensity to allow a quantitative extraction of the data.

3. Results

In Fig. 2 we show an electron spectrum acquired by focusing a 5×10^{19} W/cm^2 laser pulse on a 2 μm-thick Ti foil. The electron temperature derived from the data was about 1.4 MeV and the analysis of the image plate stacks (Fig. 3) gave a similar value. The divergence derived for the stack data was $\approx$0.5 rad, with slightly better collimation for the higher energy electrons.

Fig. 4 shows a typical recorded spectral image. It was acquired by focusing a laser pulse with an intensity of 5×10^{19} W/cm^2 on a 2 μm-thick Ti foil (the horizontal and the vertical directions correspond to the energy and the spatial extent of the emission, respectively). Due to the 1D imaging the spectra are integrated over the extension of the plasma along the line of sight. The two intensity peaks are the $K_{\alpha 1}$ and $K_{\alpha 2}$ lines, as indicated by the arrows. A lineout in the vertical direction provides the dimension of the source; in this case, an FWHM of about 60 μm on target is measured.

In Fig. 5 we show a comparison between polarized and non-polarized spectra for different target thicknesses. The non-polarized spectra show an increasingly pronounced shoulder on the "blue" sides of both $K_{\alpha 1}$ and $K_{\alpha 2}$ as the target thickness is decreased, as has been already noted in Ref. [15]. For the polarized spectra the change is considerably more pronounced than for the non-polarized ones. For the 2-μm and 5-μm thicknesses the blue side is so strongly enhanced that $K_{\alpha 2}$ becomes a small bump on the red side of $K_{\alpha 1}$.

Fig. 6 shows a dependence of both polarized and non-polarized spectra on the displacement from the peak-emission position of 12, 24, and 36 μm, for a 2 μm-thick target. The spatial resolution was 4 μm, and the laser intensity was 5×10^{19} W/cm^2. It is seen that at the peak intensity there is a clear difference between the polarized and non-polarized spectra. At 24 μm from the maximum, the difference becomes smaller: the blue wing of the polarized spectrum is significantly reduced towards the unpolarized wing. At 36 μm from the maximum the two spectra nearly coincide within the experimental error-bars.

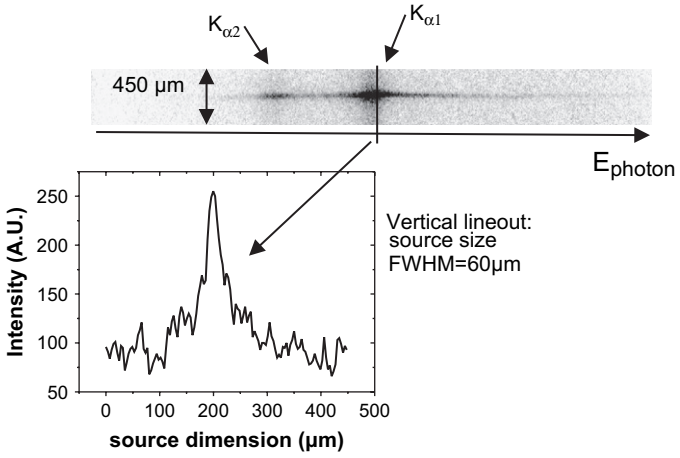

Fig. 4. A typical spectral image with 12 laser pulses and without polarizer for a laser intensity of 5×10^{19} W/cm^2 on a 2 μm-thick Ti foil target. A vertical scan of the film (denoted as "lineout") at the $K_{\alpha 1}$ peak position is shown.

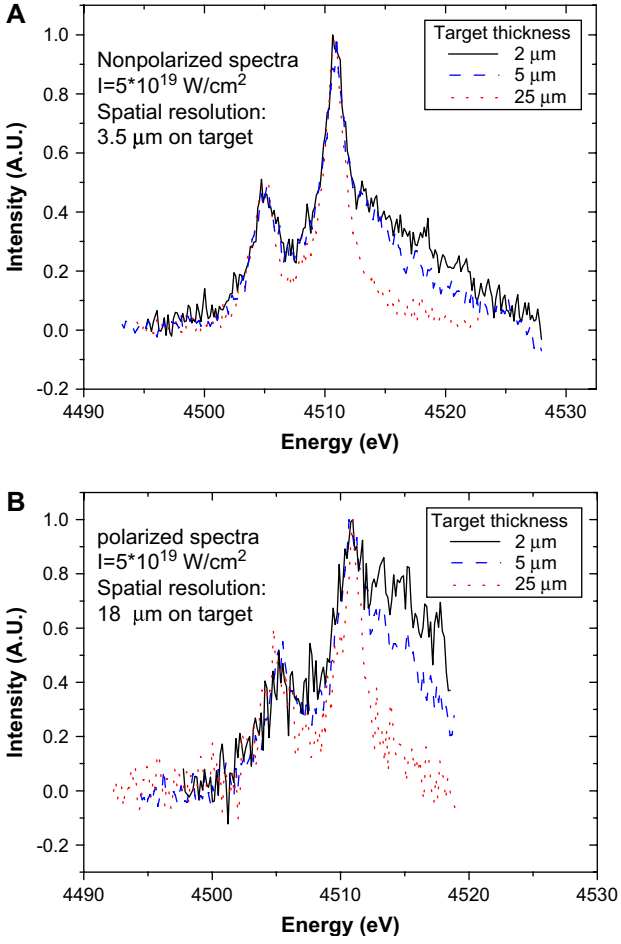

Fig. 5. Comparison of polarized and non-polarized spectra for different target thickness in the region of maximum intensity. The lower spatial resolution in (B) was required to increase the signal to noise ratio (color in online).

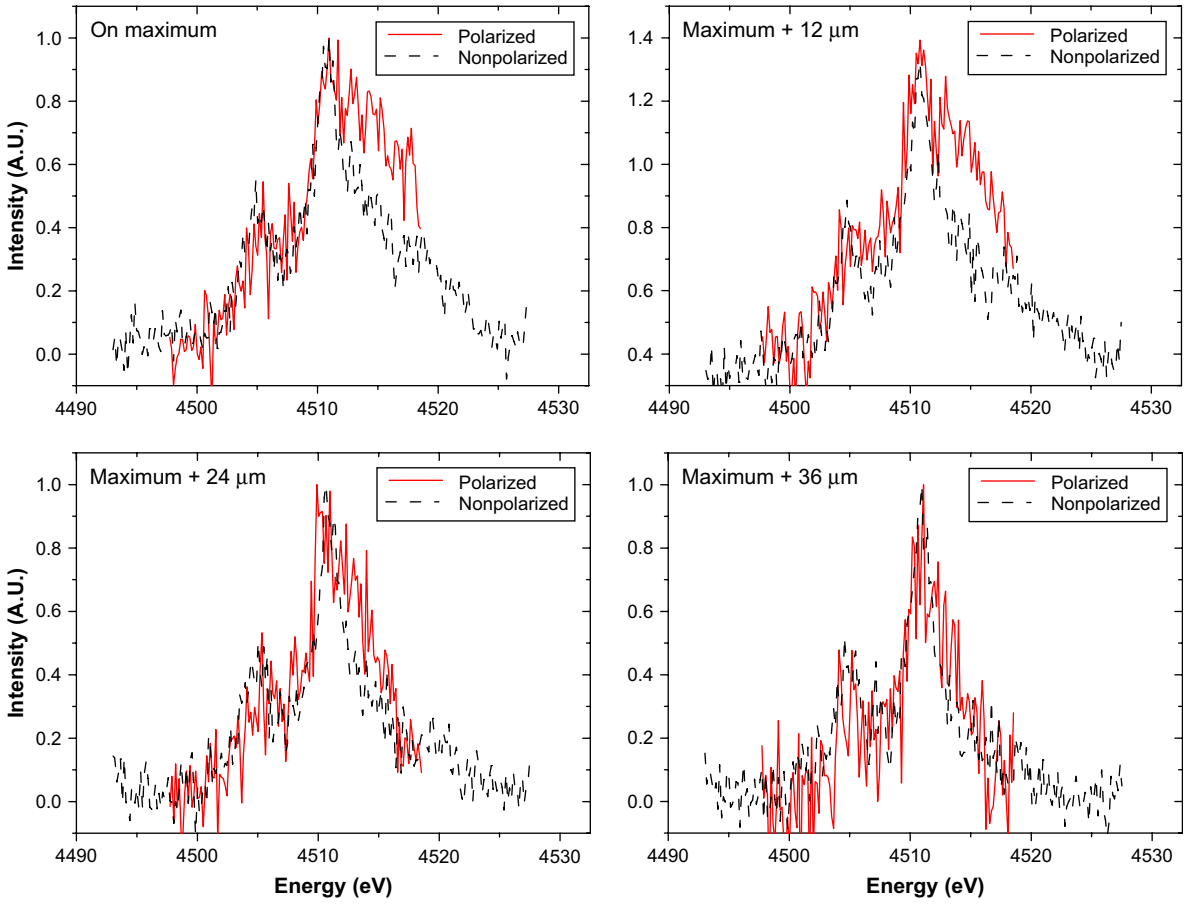

Fig. 6. The dependence of the measured K_α spectra on the displacement from the position of the maximum intensity (color in online).

These results may provide insight into the electron motion within the target. The beam-like feature of the electron velocity distribution, clearly visible in the stack analysis, spreads out significantly only about 20 μm away from the laser focal spot; 40 μm away from focus the electron distribution is nearly isotropic. We note that the target in the spectra in Fig. 6 was only 2 μm thick and the laser focal spot 5 μm^2. The region over which the electron velocity distribution stays anisotropic is much larger than these dimensions. It is possible that this is caused by the inhibition of electron propagation due to electric fields [16]. The bending of electron trajectories due to magnetic fields [17] may also have played a role.

4. Conclusions

We measured spectra of the K_α emission from Ti foil targets irradiated by femtosecond laser pulses. A strong polarization dependence of the X-ray spectra was observed. The polarized spectrum evolution as a function of the distance from the peak of the emitted intensity was determined with a 4-μm spatial resolution. The results present a clear indication of strongly anisotropic processes *inside* the laser-irradiated targets, and thus can be used, e.g., in the studies of electron transport properties under such extreme conditions of relativistic plasmas at solid density.

Acknowledgements

This work was partially supported by the German-Israeli Project Cooperation, Foundation (DIP), by the Deutsche Forschungsgemeinschaft (project B6 in Sonderforschungsbereich SFB-TR 18) and Laserlab Europe.

References

[1] T. Fujimoto, S.A. Kazantsev, Plasma Phys. Control. Fusion 39 (1997) 1267.
[2] J.C. Kieffer, J.P. Matte, H. Pépin, M. Chaker, Y. Beaudoin, T.W. Johnston, C.Y. Chien, S. Coe, G. Mourou, J. Dubau, Phys. Rev. Lett. 68 (1992) 480.
[3] J.C. Kieffer, J.P. Matte, M. Chaker, Y. Beaudoin, C.Y. Chien, S. Coe, G. Mourou, M.K. Inal, Phys. Rev. E 48 (1993) 4648.
[4] A.S. Shlyaptseva, R.C. Mancini, P. Neill, P. Beiersdorfer, Rev. Sci. Instrum. 68 (1997) 1095.
[5] P. Beiersdorfer, G. Brown, S. Utter, P. Neill, K.J. Reed, A.J. Smith, R.S. Thoe, Phys. Rev. A 60 (1999) 4156.
[6] A.S. Shlyaptseva, D.A. Fedin, S.M. Hamasha, S.B. Hansen, C. Harris, V.L. Kantsyrev, P. Neill, N. Ouart, P. Beiersdorfer, U.I. Safronova, Rev. Sci. Instrum. 74 (2003) 1947.
[9] F. Pisani, A. Bernardinello, D. Batani, A. Antonicci, E. Martinolli, M. Koenig, L. Gremillet, F. Amiranoff, S. Baton, J. Davies, T. Hall, D. Scott, P. Norreys, A. Djaoui, C. Rousseaux, P. Fews, H. Bandulet, H. Pepin, Phys. Rev. E 62 (2000) 5927.
[10] L. Romagnani, J. Fuchs, M. Borghesi, P. Antici, P. Audebert, F. Ceccherini, T. Cowan, T. Grismayer, S. Kar, A. Macchi, P. Mora, G. Pretzler, A. Schiavi, T. Toncian, O. Willi, Phys. Rev. Lett. 95 (2005) 195001.

[11] T. Feurer, W. Theobald, R. Sauerbrey, I. Uschmann, D. Altenbernd, U. Teubner, P. Gibbon, E. Förster, G. Malka, J.L. Miquel, Phys. Rev. E 56 (1997) 4608.
[12] K.B. Wharton, S.P. Hatchett, S.C. Wilks, M.H. Key, J.D. Moody, V. Yanovsky, A.A. Offenberger, B.A. Hammel, M.D. Perry, C. Joshi, Phys. Rev. Lett. 81 (1998) 822.
[13] Ch. Ziener, I. Uschmann, G. Stobrawa, Ch. Reich, P. Gibbon, T. Feurer, A. Morak, S. Düsterer, H. Schwoerer, E. Förster, R. Sauerbrey, Phys. Rev. E 66 (2002) 066411.
[14] I. Uschmann, E. Förster, K. Gäbel, G. Hölzer, M. Ensslen, J. Appl. Cryst. 26 (1993) 405.
[15] S.B. Hansen, A.Ya. Faenov, T.A. Pikuz, K.B. Fournier, R. Shepherd, H. Chen, K. Widmann, S.C. Wilks, Y. Ping, H.K. Chung, A. Niles, J.R. Hunter, G. Dyer, T. Ditmire, Phys. Rev. E 72 (2005) 036408.
[16] A.R. Bell, J.R. Davies, S. Guerin, H. Ruhl, Plasma Phys. Control. Fusion 39 (1997) 653.
[17] Ch. Reich, I. Uschmann, F. Ewald, S. Düsterer, A. Lübcke, H. Schwoerer, R. Sauerbrey, E. Förster, P. Gibbon, Phys. Rev. E 68 (2003) 056408.